Microstructure and Steel Rail Shelling Resistance

H. P. LIEURADE*, K, DANG VAN** and N. JI***
IRSID – Saint-Germain-en-Laye, France
***Ecole Polytechnique – Palaiseau, France*
****ENSAM – Paris, France*

ABSTRACT

A type UIC 900 A steel used for rail was subjected to different types of heat treatment corresponding to different colling rate after austenitizing.

This study enabled the influence of microstructures on low cycle fatigue characteristics X-ray diffraction measurements have been use to evaluate the cyclic cold work.

The second part of the study, which consists of a theoretical modelling of shelling using behaviour laws determined experimentally, showed the benefits of refining steel microstructure in order to increase rail fatigue life.

INTRODUCTION

During service, rails are subjected to increasingly severe mechanical loading caused by the gradual increase of loads caused by axles and train speeds.

In order to prevent or delay rail damage during service, the use of steel grades with improved properties is required.

These improved grades can be obtained in either of two ways. Steel-makers offer microalloyed grades (Cr, V, etc) in as-rolled condition, or mechanical properties are improved by heat treatment of the rail in order to obtain a finer perlitic structure than that present in the as-rolled condition.

The latter method enables high mechanical strength to be combined with great toughness.

As a result of progress made by steelmakers in the area of improving steel properties, transverse cracking of rail ("tache ovale") has almost completely disappeared. However, shelling and gradual wear of railheads are a problem.

The present study determines the cyclic behaviour laws governing the same steel grade subjected to different types of heat treatment and evaluates the fatigue life corresponding to the appearence of shelling in the absence of wear.

X-ray diffraction measurements enable more detailed analysis of cyclic behaviour of the conditions studied to be performed through examination of the simultaneous changes in residual stress and cold work in the ferritic phase.

EXPERIMENTAL CONDITIONS

Material

Table 1 gives the chemical composition of the grade studied (UIC 900 A).

Table 1 : Chemical Composition (in 10^{-3} %)

C	Mn	P	S	Si	Al	Ni	Cr	Cu
693	1036	25	19	348	10	41	22	18

Cylinders with a diameter of 30 mm and a length of 1150 mm were austenitized at 820°C and then cooled. Three types of cooling process were used in order to obtain fine perlite microstructure with varying perlite interlamellar spacing :

- Item A : slow cooling in a furnace at 80°C,
- Item B : blown air cooling,
- Item C : lead bath cooling at 415°C.

The perlite interlamellar spacing was measured in each case using a scanning electron microscope (SEM) for observations at enlargements of 5,000 or 10,000.

The average interlamellar spacing was calculated using enlarged photos (1 to 3).

Table 2 gives tensile properties and average interlamellar distances (d_m). Real stress at breaking (σ_f) and the cold work coefficient (n) are given for each case.

Table 2 : Tensile Properties

Item	σ_y (MPa)	UTS (MPa)	σ_f (MPa)	Elong. (%)	R.A. (%)	n	d_m (µm)
A	445	905	1252	17.7	35.5	0.130	0.390
B	575	1030	1502	15.9	43.6	0.124	0.295
C	705	1100	1612	14.7	44.3	0.116	0.205

Test Method

The low cycle fatigue tests were carried out under total strain range control specimen (Ø 8 mm, L = 10 mm) deformation. The geometrical characteristic of the specimen are 8 mm diameter and 10 mm gage length.

For each test, the triangular loading cycle corresponded to a deformation speed of $\dot{\epsilon} = 4.10^{-3}$/second.

The properties of the stable cycle were measured or calculated for a fatigue life equivalent to half the rupture life (N_R).

LOW CYCLE FATIGUE TEST RESULTS

Low Cycle Fatigue Resistance

The test results enabled the coefficients for the Basquin and Manson-Coffin equations to be determined. These coefficients are given in Table 3.

Cyclic Curves

Figure 1 shows the linear and cyclic tensile curves for the three metallurgical states studied. The cyclic yield strength (σ'_y) and the coefficients (n' and k') of the cyclic cold work law are given in Table 3.

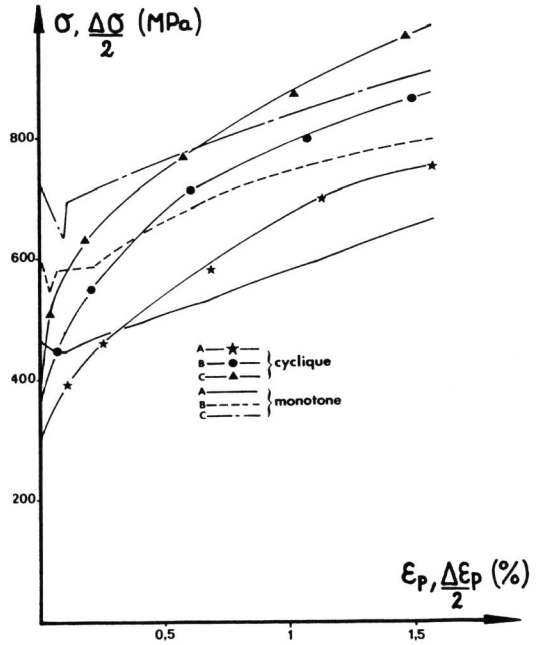

Figure 1 : Monotonic and Cyclic curves.

Table 3 : Cyclic Properties

Item	b	c	σ'_f/E (%)	ϵ'_f	σ'_y (MPa)	n'	k' (MPa)
A	- 0.22	- 0.51	1.62	33	308	0.26	2220
B	- 0.20	- 0.58	1.66	50	368	0.22	2150
C	- 0.16	- 0.58	1.38	48	400	0.19	2100

THEORETICAL APPROACH

Modelling the shelling mechanism required accurate knowledge of the stress and strain fields and their development as wheels travel over the rails.

Modelling Principle

This type of modelling has been described already (4) ; the principles underlying two-dimensional modelling are :

- a calculation method based on the finite element method with the rail being assimilated as a very long strip ; the transverse thickness is great enough to retain the hypothesis of plain strain ;
- the stabilized stress and deformation state is obtained after a certain number of wheel passages ; this number varies, but is usually around ten ;
- a linear kinematic behaviour law is used, as can be seen from the results of the low cycle fatigue tests ;
- in each case, modelling can be used to determine the maximum equivalent deformation value ($\Delta\epsilon_{eq}$) corresponding to the passage of an axle :

$$\Delta\epsilon_{eq} = \underset{t_i}{\text{Max}} \; \underset{t}{\text{Max}} \left[\frac{2}{3} \{\epsilon_{ij}(t) - \epsilon_{ij}(t_i)\} \{\epsilon_{ij}(t) - \epsilon_{ij}(t_i)\} \right]^{1/2}$$

- the Manson-Coffin laws are applied directly once $\Delta\epsilon_{eq}$ has been determined ;
- in all cases, rail wear is assumed to be non-existent.

Mechanical Parameters Examinated

- Maximum Pressure

Calculations were performed for the various maximum Hertz pressure values (p_o) and led to an accomodated loading in all cases. Values for the ratio p_o/τ_e between 4, 5 and 6 (τ_e = yield strength for shear) were used since they correspond to realistic loading parameters (4).

- Friction Coefficient

The existence of dry friction was taken into account by assuming that tangential loads (q_o) were proportional to normal loads in the coefficient ratio f ($q = f.p_o$).

Shelling Resistance

Theoretical evaluation of the scalling resistance of the three states studied was performed assuming that rail wear was non-existent.

Under this assumption, figure 2 shows the development of the fatigue life at initiation (N) as a function of p_o/τ_e for two different friction coefficient values : 0 and 0.2.

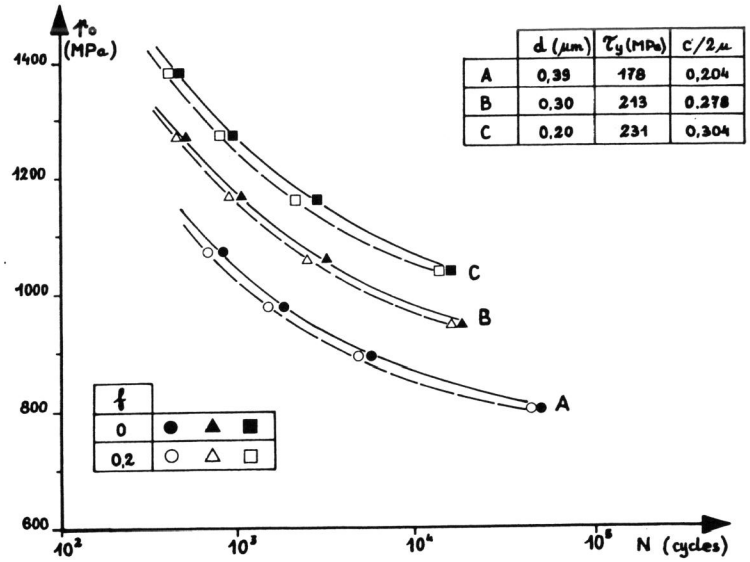

Figure 2 : Fatigue life vs maximum pressure (p_o) as a function of friction coefficient (f).

DISCUSSION

Low Cycle Fatigue Resistance

Figures 3a and 3c respectively compare the "elastic" lines, the "plastic" lines and the total deformation curve.

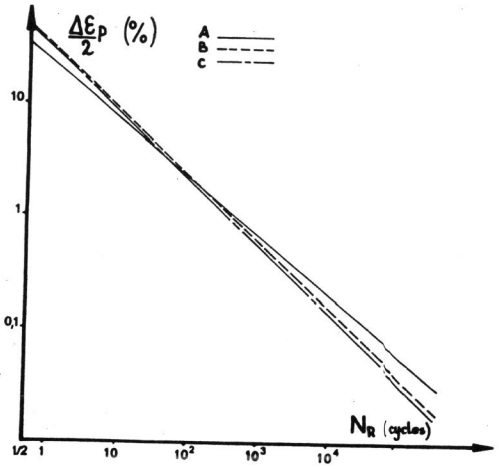

a) Plastic curves $\frac{\Delta\epsilon}{2}p$ vs N_R.

b) Elastic curves $\frac{\Delta\epsilon}{2}e$ vs N_R.

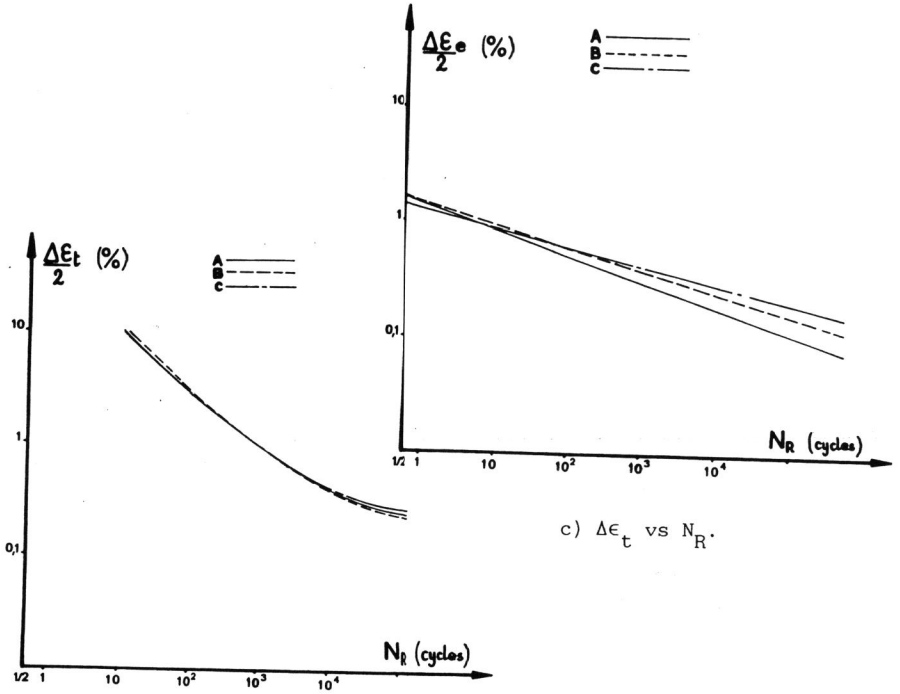

c) $\Delta\epsilon_t$ vs N_R.

Figure 3 : Low cycle fatigue resistance.

The "elastic" lines are classified in the same order as the yield strength levels. State C, which has the finest microstructure, has the best behaviour.

The plastic lines are classified in the opposite order, in accordance with the classification of elongation properties.

The total deformation curves are very similar.

Cyclic Behaviour Laws

The three metallurgical states studied show cyclic softening for the plastic strain low amplitudes. Figure 1 shows a drop in the proportional limit after cyclic loading and a softening that is greater when initial properties are high (state C) and in a field of $\frac{\Delta\epsilon}{2}p$ which increases with σ_y. This softening phenomenon leads, for low $\frac{\Delta\epsilon}{2}p$, to a lower deviation between the cyclic curves than that observed between linear curves, while staying within the classification obtained during linear loading tests.

This result confirms the works of Sunwoo et al. (5) and those of Dang van et al. (4).

Measurement of the Cyclic Cold Work

X-ray diffraction measurements were made of the test specimens after testing, excluding the fracture surface. These measurements were only made in the ferritic phase ; therefore the obtained results are not mean values of the residual stresses existing in the material. These results revealed the following (Figure 4) :

- the level of residual stress (σ_R) increases when $\Delta\epsilon$ increases (N_R decreases)
- the diffraction peak breadth, related to the cold working in the ferritic phase, increases slightly when $\Delta\epsilon$ increases (N_R decreases).
- the evolution of σ_R becomes lower the finer the perlite structure ;
- the peak breadth is correlated with the stress amplitudes measurements on the stabilized cycles, $\frac{\Delta\sigma}{2}$ (figure 4c). It slightly increases with $\frac{\Delta\sigma}{2}$.
- the low cold working evolution, evaluated by diffraction peak breadth, covers a major cold working gradient in the ferritic phase.

Effect of the Microstructure on Shelling Resistance

Figure 2 shows a marked improvement in theoretical shelling resistance when microstructure is finer.

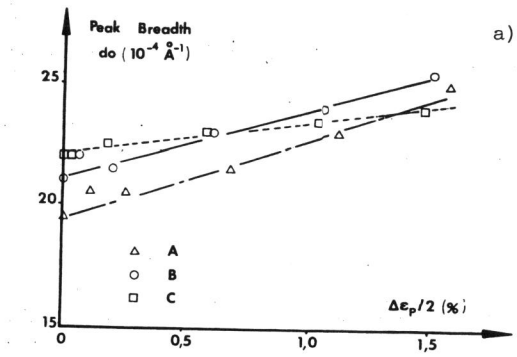

a) peak breadth vs $\Delta\epsilon_p/2$.

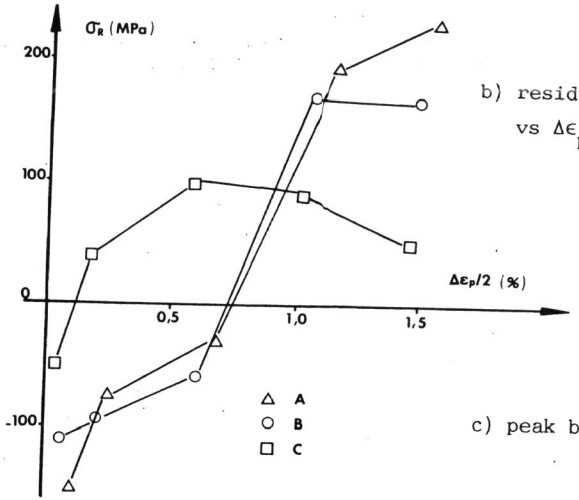

b) residual stresses (σ_R) vs $\Delta\epsilon_p/2$.

c) peak breath vs $\frac{\Delta\sigma}{2}$.

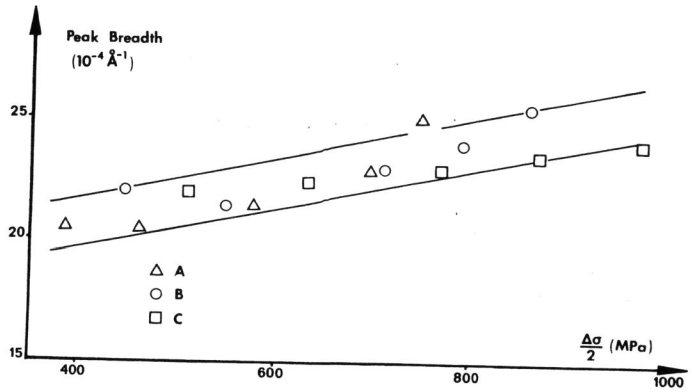

Figure 4 : X-Ray diffraction measurements.

For example, for a maximum pressure (p_o) of 1000 MPa, fatigue life is respectively multiplied by 5 and by 20 when the average interlamellar spacing increases from 0.20 to 0.30 and from 0.20 to 0.39.

For a fatigue life of close to 10^4 cycles, the maximum pressure increases by approximately 15 and 25 % respectively.

CONCLUSION

Refining the microstructure of a grade 900 A rail steel after different cooling methods are used leads to :

- improved linear tensile properties of the metal, in particular yield strength and ductility (Reduction in Area),
- significantly improved steel cyclic properties.

Theoretical calculations performed without taking wear into account showed that this improvement results in a significant increase in shelling resistance.

REFERENCES

(1) Takahashi T. et coll. (1970). Trans. J.I.M., vol. 11, p. 113-119.

(2) Nack N.J. et coll. (1986). Mat. Sci and Engin., vol. 83, p. 145-149.

(3) O'Donnelly B.E. et coll. (1986). Mat. Sci. and Engin., vol. 84, p. 131-135.

(4) Dang Van K., Derboule B., Deroche R.Y., Conti R., Lieurade H.P. (1987). Etude du mécanisme de formation de l'écaillage des rails. Mem. Scient. Rev. Metallurgie, Juillet, Août, P.363-374.

(5) Sunwoo H., Fine M.E., Meskil M., Stone D.H. (1982). Cyclic deformation of pearlitic eutectoïd rail steel. Met. Trans. A. Vol. 13A - nov., p. 2036-2047.